DMD Fast Forward. Published on September 29, 2008 as doi:10.1124/dmd.108.021477

DMD #21477

TITLE PAGE

The multiple depletion curves method provides accurate estimates of CL_{int}, V_{max}, and K_m: Accuracy and robustness evaluated through experimental data and Monte Carlo simulations

Erik Sjögren, Hans Lennernäs, Tommy B. Andersson, Johan Gråsjö and Ulf Bredberg

Department of Pharmacy, Uppsala University, BOX 580, S-751 23 Uppsala, Sweden (E.S., H.L., J.G.); Clinical Pharmacology and DMPK, AstraZeneca R&D, Mölndal, Sweden (T.A.); Section of Pharmacogenetics, Department of Physiology and Pharmacology, Karolinska Institutet, Stockholm, Sweden (T.A.); Discovery DMPK&Bioanalytical Chemistry, AstraZeneca R&D, Mölndal, Sweden (U.B.)

RUNNING TITLE PAGE

a)
Running title: Accurate estimation of enzyme kinetics from depletion data

b)
Corresponding Author:
Hans Lennernäs, PhD, Professor in Biopharmaceutics
Department of Pharmacy
Uppsala University
Box 580
SE-751 23 Uppsala
Sweden

E-mail: hans.lennernas@farmaci.uu.se
Telephone: +46 18 471 4317
Fax: +46 18 471 4223

c)
Text pages: 31
Tables: 3
Schemes: 0
Figures: 7
References: 28
Abstract: 222 words
Introduction: 749 words
Discussion: 1681 words

d)

Nonstandard abbreviations: MDCM, multiple depletion curves method; IFRMM, initial formation rate of metabolite method; $T_{½}M$, "*in vitro* $t_{½}$" method; EAC, enzyme-activity-change; CYP, cytochrome P450; FLU, flutamide; RES, resorufin; ERES, ethoxyresorufin; BRES, benzyloxyresorufin; DFN, diclofenac; DXM, dextromethorphan; 2FLU, 2-OH-flutamide; DXO, dextrorphan; 4DFN, 4'-OH-diclofenac; EMEL, ethylmelagatran; NMEL, N-hydroxymelagatran; MEL, melagatran; HPLC, high performance liquid chromatography; LC, liquid chromatography; LLOQ, lower limit of quantitation; UV, ultraviolet; FL, fluorometric; MS, mass spectrometry;

Abstract:

The use of multiple depletion curves for the estimation of V_{max}, K_m and CL_{int} was thoroughly evaluated by means of experimental data and through a series of Monte Carlo simulations. The enzyme kinetics of seven compounds were determined using the multiple depletion curves method (MDCM), the traditional initial formation rate of metabolite method (IFRMM) and the "*in vitro* $t_{½}$" method and the parameter estimates derived from the three methods were compared. The impact of a change in enzyme activity during the incubation period on the parameter estimates and the possibility to correct for this was also investigated. The MDCM was in good overall agreement with the IFRMM. Correction for a change in enzyme activity was possible and resulted in a better concordance in CL_{int} estimates. The robustness of the method in coping with different rates of substrate turnover and variable starting concentrations was also demonstrated through Monte Carlo simulations. Further, the limitations imposed by assumptions inherent in the "*in vitro* $t_{½}$" method were demonstrated both experimentally and by simulations. This study demonstrates that the MDCM is a robust and efficient method for estimating enzyme kinetic variables with high accuracy and precision. The method may potentially be used in a wide range of applications, from pure enzyme kinetics to *in vitro*-based predictions of the pharmacokinetics of compounds with multiple and/or unknown metabolic pathways.

Estimation of metabolic intrinsic clearance (CL_{int}) is currently included in many drug discovery programs. The most frequently used assay is the "*in vitro* $t_{½}$" method ($T_{½}M$), in which CL_{int} is derived from the monoexponential slope of a single depletion curve (Obach, 1999). This method is used both for ranking compounds with respect to metabolic stability and for the prediction of metabolic clearance in animals and humans. The data are usually obtained from incubations with microsomes or fresh or cryopreserved hepatocytes (Iwatsubo et al., 1997; Obach et al., 1997; Rodrigues, 1997; Ito and Houston, 2005). CL_{int}, defined as the maximum velocity of the metabolic reaction (V_{max}) divided by the Michaelis constant (K_m), the substrate concentration that yields half of V_{max}, is by this means used as the link between fundamental enzyme kinetics and *in vivo* pharmacokinetic variables (Rane *et al*., 1977). Although the $T_{½}M$ approach is fast, it is built on the assumption that the initial concentration (C_0) is well below K_m. This assumption is often valid but if not, the method will underestimate CL_{int} and thus underpredict the rate of hepatic clearance *in vivo*. The basic assumption of $C_0 << K_m$ is usually not confirmed and may be one of several contributing factors to the tendency of systematic underprediction of hepatic clearance seen in the literature (Carlile *et al*., 1999; Obach, 1999; Ito and Houston, 2005). The ability to predict clearance via an estimate of CL_{int} is nevertheless good and the method has frequently shown its value (Rostami-Hodjegan and Tucker, 2007). One shortcoming, however, is the fact that CL_{int} is a secondary parameter reflecting a simplified picture of metabolic capacity with no information of the underlying primary parameters, V_{max} and K_m. The confident quantification of these parameters for specific reactions could improve the assessment of drug-drug interactions, help define the contributions of individual metabolic pathways and predict inter-individual variability caused by genetic polymorphism. Assessment of K_m in combination with CL_{int} enables the prediction of non-linear kinetics (concentration and dose-dependent bioavailability and clearance) which may improve the accuracy of the prediction

of *in vivo* pharmacokinetics. Knowledge of both CL_{int} and K_m for drug candidates as well as for selected compounds in lead optimization is therefore of great value (Ludden, 1991; Obach and Reed-Hagen, 2002).

The traditional method used for the determination of V_{max} and K_m for a specified reaction is the initial formation rate of metabolite method (IFRMM) where the Michaelis-Menten equation is fitted to the initial formation rates of metabolite at different substrate concentrations. To obtain the total CL_{int}, V_{max} and K_m for all individual metabolic pathways need to be estimated. However, many drug compounds are metabolized at multiple positions and for new chemical entities these are usually not identified early in the discovery process. These two factors make the method inappropriate for enzyme kinetic investigations in drug discovery. An alternative approach was suggested where parent compound depletion curves at multiple concentrations are generated. V_{max} and K_m are then estimated by fitting the Michaelis-Menten equation to all disappearance curves simultaneously (Bousquet-Melou *et al*., 2002). This method is better suited for investigations of enzyme kinetics in drug discovery but it has not yet been thoroughly evaluated. In contrast to the $T_{½}M$, the method generates information of the potential for non-linear pharmacokinetics behavior and does not rely on the assumption of $C_0 << K_m$, reducing the risk for under estimation of CL_{int}. However, both methods involve extended incubation times compared to the IFRMM, raising the potential for enzyme degradation and/or inhibition effects during the incubation period (Houston and Carlile, 1997; Jones and Houston, 2004). This could be accounted for by including an enzyme-activity-change (EAC) variable in the kinetic model used in the regression analysis (Bousquet-Melou *et al*., 2002).

The main objective of this study was to evaluate the multiple depletion curves method (MDCM) by comparing the results (V_{max}, K_m, CL_{int}) with those gained by the IFRMM and the

$T_{½}M$. A secondary aim was to investigate the impact of change in enzyme activity on the estimates obtained from depletion based methods and the possibility to correct for such effects in the data analysis. In this report, we examined seven metabolic reactions in either rat liver microsomes or porcine liver S1 fractions. The data enabled a direct comparison of the MDCM, the IFRMM and the $T_{½}M$. Monte Carlo simulation analyses were performed in order to further investigate the robustness, accuracy and sensitivity of the MDCM. Similar analyses were performed for investigation of the $T_{½}M$ and the impact of a change in enzyme activity during the incubation period.

Materials and Methods

Materials

The following substrates (short name in parentheses), metabolites and internal standards were obtained from Sigma-Aldrich (Schnelldorf, Germany): flutamide (FLU), carbamazepine, resorufin (RES), ethoxyresorufin (ERES), benzyloxyresorufin (BRES), diclofenac (DFN), N-phenylanthranilic acid, dextromethorphan (DXM). 2-OH-flutamide (2FLU) was obtained from Mikromol (Luckenwalde, Germany). Dextrorphan (DXO) and 4'-OH-diclofenac (4DFN) were purchased from BD Gentest corp. (Woburn, MA). Ethylmelagatran (EMEL), N-hydroxymelagatran (NMEL) and melagatran (MEL) were a kind gift from AstraZeneca (Mölndal, Sweden). All other reagents and chemicals were of appropriate grade and purchased from Sigma Chemicals.

Compound selection and enzyme sources

To enable a valid comparison between the MDCM and the IFRMM, it was important to account for the majority of the metabolic routes. Substrates were therefore selected based on the criteria of a maximum of two dominating measurable metabolic routes contributing to at least 80% of the total metabolism. Ideally, CL_{int}, V_{max} and K_m should also cover a wide range. The following seven substrates were selected and corresponding metabolites were used for determination of V_{max} and K_m by the traditional IFRMM: BRES O-dealkylation to RES mediated by CYP1A2 and CYP2B1 (Kobayashi *et al*., 2002), DFN 4-hydroxylation to 4DFN mediated by CYP2C6 (Kobayashi *et al.*, 2002), DFN 5-hydroxylation to 5-OH-diclofenac (5DFN) mediated by multiple CYPs (Tang *et al*., 1999), DXM O-demethylation to DXO mediated by CYP2D2 (Kobayashi *et al*., 2002), ERES O-deethylation to RES mediated by CYP1A2 and CYP2C6 (Kobayashi *et al*., 2002), EMEL ester hydrolysis to MEL (specific

enzymatic pathway unidentified) (Eriksson *et al*., 2003), FLU 2-hydroxylation to 2FLU mainly mediated by CYP1A2 (Berson *et al*., 1993; Fau *et al*., 1994) and NMEL reduction to MEL (specific enzymatic pathway unidentified) (Eriksson *et al*., 2003). The reactions are displayed in Figure 1.

All reactions were investigated in female rat liver microsomes except for EMEL and NMEL where male porcine liver S1 fractions were used in order to include all enzymes involved in the metabolism of these compounds (Clement and Lopian, 2003). The female rat liver microsome fractions were a kind gift from AstraZeneca (Mölndal, Sweden). Liver S1 fractions were prepared as follows; fresh male porcine (Swedish landrace) liver was flushed with ice cold isotonic saline solution to remove blood and to cool the tissue. Pieces of the liver were homogenized in ice cold KPO_4 buffer (0.1 M, pH 7.4) (1:5 v/w) with a ULTRA-TURRAX dispersion unit for 30 sec at 6500 rpm and then centrifuged at 1000 g for 10 minutes. The supernatant was collected as the S1 fraction and used within four hours to minimize the risk of enzyme degradation. Preparations were conducted on ice in an 8°C refrigerated room and S1 fractions were kept on ice until use. Total protein concentration was determined using a Quick Start Bradford kit (Bio Rad Laboratories AB, Sundbyberg, Sweden) with immunoglobulin as a reference protein.

General incubation conditions and sample treatment

All incubations were conducted shaking under air at 37˚C. The incubation matrices consisted of KPO_4 buffer (final concentration 0.1 M, pH 7.4) and selected cell fractions at optimal protein concentration for the respective substrates. Incubations were performed by adding the substrate to the matrix. The reaction was started after five minutes equilibration by adding

NADPH to a final concentration of 1 mM. The concentration of organic solvent did not exceed 0.5% in any of the incubations. After termination, samples were centrifuged for 10 minutes at 10000 g (Minispin^{plus}, Eppendorf, Germany) and an aliquot of the supernatant was drawn for sample analysis. When necessary, the aliquot was mixed with water or buffer to mimic the mobile phase of the analytical method. The substrate concentration range investigated in the metabolic assays was limited by the solubility and lower limit of quantitation (LLOQ) of the analytical method for each substrate. Product formation experiments and substrate depletion experiments were conducted in triplicate and sets of five, respectively.

Investigations of linearity between the initial rate of metabolism and protein concentration were examined in the protein concentration interval 0.125 – 0.75 mg protein /ml. The protein concentration and incubation time chosen for each substrate was based both on linearity and a maximum substrate depletion of 15%. Optimal protein concentration and time points for sampling are given for respective substrates in the metabolic assay section.

Enzyme stability during incubation conditions was studied by comparing measurements of the initial reaction velocity after 3, 33 and 63 minutes of incubation stress. At time point 0, reaction tubes containing enzyme in KPO_4 buffer (0.1 M, pH 7.4) were placed in a heated water bath at 37˚C. Substrates were added at times 0, 30 and 60 minutes and the reactions was initiated after 3 minutes of pre-incubation, i.e. 3, 33 and 63 minutes, by the addition of cofactor to a final concentration of 1 mM. Time points for sample withdrawal, protein concentration and sample treatment were as described in the metabolic assay for each substrate.

Protein binding in the incubation media was determined by adding different amounts of substrate to 1 ml of incubation medium (enzyme and 0.1 M KPO_4 buffer, pH 7.4) covering a suitable range of concentrations. After 10 minutes of equilibrium, samples of 100 µl were drawn to measure the total concentration. The remaining medium was separated from proteins and other cellular material by ultrafiltration (10000 g for 20 minutes) using a YM – 10 Microcon filter, cut off 10000 MW (Millipore, Solna, Sweden). The filtrate was analyzed to measure the unbound concentration. To determine unspecific binding to the filter, concentrations were measured in filtered and unfiltered 0.1 M KPO_4 buffer, pH 7.4. Other binding to the device (e. g. internal walls) was assumed to be negligible as no significant binding to other experimental equipment was observed. All samples were treated as described in the metabolic assay for each substance. The following concentration ranges were investigated: BRES 0.020-1.5 µM; DFN 10-100 µM; DXM 0.15-15 µM; EMEL 7.5-750 µM; ERES 0.020-2.0 µM; NMEL 12-1200 µM and FLU 1-30 µM.

Chemical stability in incubation medium (enzyme and 0.1 M KPO_4 buffer, pH 7.4) under incubation conditions was examined by keeping the substance in incubation medium at 37°C. Samples were removed at 0, 20, 40 and 60 minutes and treated as described in the metabolic assay for each substance.

Metabolic assays

BRES metabolism

Rat liver microsomes at a final concentration of 0.5 mg/ml were used for BRES assays. Product formation experiments for BRES (23-2500 nM) were conducted for 13.5 minutes and samples of 100 µl were drawn at 0, 4.5, 9 and 13.5 minutes. Substrate depletion experiments for BRES (20-2000 nM) were performed for 60 minutes and samples of 50 µl were removed

at 0, 5, 10, 15, 20, 30, 40, 50 and 60 minutes. The reactions were terminated by adding an equivalent of three sample volumes of ice cold methanol containing ERES as internal standard. Samples were centrifuged and the supernatant was then injected into the high performance liquid chromatography (HPLC) system.

DFN metabolism

Rat liver microsomes at a final concentration of 0.5 mg/ml were used for DFN assays. Product formation experiments for DFN (1.9-440 µM) were conducted for 13.5 minutes and samples of 100 µl were drawn at 0, 4.5, 9 and 13.5 minutes. Substrate depletion experiments for DFN (3.5-350 µM) were performed for 60 minutes and samples of 100 µl were removed at 0, 7.5, 15, 22.5, 30, 37.5, 45, 52.5 and 60 minutes. The reactions were terminated by adding 200 µl CH_3CN containing N-phenylanthranilic acid as internal standard. Post-centrifugation supernatant aliquots were mixed with an equal amount sodium acetate buffer (0.75 mM, pH 5.0) before analysis by HPLC.

DXM metabolism

Rat liver microsomes at a final concentration of 0.5 mg/ml were used for DXM assays. Product formation experiments for DXM (0.1-60 µM) were conducted for 13.5 minutes and samples of 100 µl were drawn at 0, 4.5, 9 and 13.5 minutes. Substrate depletion experiments for DXM (0.5-50 µM) were performed for 60 minutes and samples of 100 µl were removed at 0, 7.5, 15, 22.5, 30, 37.5, 45, 52.5 and 60 minutes. The reactions were terminated by adding 350 µl stop solution (CH_3CN, methanol, phosphoric acid, 17:17:4) containing DFN as internal standard. Samples were centrifuged and the supernatant was then injected into the HPLC system.

ERES metabolism

Rat liver microsomes at a final concentration of 0.125 mg/ml were used for ERES assays. Product formation experiments for ERES (23-2500 nM) were conducted for 9 minutes and samples of 100 µl were drawn at 0, 3, 6 and 9 minutes. Substrate depletion experiments for ERES (180-2500 nM) were performed for 60 minutes and samples of 50 µl were removed at 0, 5, 10, 15, 20, 30, 40, 50 and 60 minutes. The reactions were terminated by adding an equivalent of three sample volumes of ice cold methanol containing BRES as internal standard. Samples were centrifuged and the supernatant was then injected into the HPLC system.

EMEL metabolism

Porcine liver S1 fractions at a final concentration of 0.3 mg/ml were used for EMEL assays. Both NADH and NADPH at final concentrations of 1 mM were used as co-factors in the assay. In contrast to the general assay procedure, NADH and NADPH were firstly added to the incubation matrix and the reactions were started after 5 minutes of equilibration by adding EMEL. Product formation experiments for EMEL (4.0-1900 µM) was conducted for 13.5 minutes and samples of 30 µl were drawn at 0, 4.5, 9 and 13.5 minutes. Substrate depletion experiments for EMEL (8.5-1400 µM) were performed for 60 minutes and samples of 40 µl were removed at 0, 7.5, 15, 22.5, 30, 37.5, 45, 52.5 and 60 minutes. The reactions were terminated by adding 100 µl CH_3CN. Post-centrifugation supernatant aliquots were diluted with water to adjust the concentration of analytes and CH_3CN to a level compatible with the analytical method before analysis by liquid chromatography (LC).

FLU metabolism

Rat liver microsomes at a final concentration of 0.5 mg/ml were used for FLU assays. Product formation experiments for FLU (1.4-57 µM) were conducted for 15 minutes and samples of 100 µl were drawn at 0, 5, 10 and 15 minutes. Substrate depletion experiments for FLU (2.1-130 µM) were performed for 60 minutes and samples of 100 µl were removed at 0, 5, 10, 15, 20, 30, 40, 50 and 60 minutes. The reactions were terminated by adding an equivalent of three sample volumes of CH_3CN containing carbamazepin as internal standard. Post-centrifugation supernatant aliquots were mixed with an equal amount of water before analysis by HPLC.

NMEL metabolism

Porcine liver S1 fractions at a final concentration of 0.3 mg/ml were used for NMEL assays. Both NADH and NADPH at final concentrations of 1 mM were used as co-factors in the assay. In contrast to the general assay procedure, NADH and NADPH were firstly added to the incubation matrix and the reactions were started after 5 minutes of equilibration by adding NMEL. Product formation experiments for NMEL (5.0-2300 µM) were conducted for 13.5 minutes and samples of 30 µl were drawn at 0, 4.5, 9 and 13.5 minutes. Substrate depletion experiments for NMEL (21-2600 µM) were performed for 60 minutes and samples of 40 µl were removed at 0, 7.5, 15, 22.5, 30, 37.5, 45, 52.5 and 60 minutes. The reactions were terminated by adding 100 µl CH_3CN. Post-centrifugation supernatant aliquots were diluted with water to adjust the concentration of analytes and CH_3CN to a level compatible with the analytical method before analysis by LC.

Analytical assays

Instrumentation

Instrumentation for HPLC analysis with ultraviolet or fluorometric detection

The HPLC system consisted of a CMA/200 refrigerated microsampler (CMA-microdialysis, Sweden) and an LC-10AD pump (Shimadzu, Kyoto, Japan). Ultraviolet (UV) detection was performed using a Spectra 100 UV detector (Thermo Separation Products, San Jose, CA) and an FP-1520 Intelligent Fluorescence Detector (Jasco, Japan) was used for fluorometric (FL) detection. Concentrations of eluted samples were calculated by comparing the peak areas to those of internal standards (when available) by reference to a calibration curve. Data were acquired and evaluated using CSW32 integrating software (Data Apex Ltd, Prague, Czech Republic).

Instrumentation for LC analysis with mass spectrometry

The LC system consisted of an HP 1100 series LC pump and column oven (Agilent Technologies Deutschland, Waldbronn, Germany), combined with an HTS PAL injector (CTC Analytics, Zwingen, Switzerland). Mass spectrometry (MS) was performed with a triple quadrupole mass spectrophotometer, API4000, equipped with an electrospray interface (Applied Biosystems/MDS Sciex, Foster City, CA). Instrument control, data acquisition and evaluation were performed using Applied Biosystems/MDS Sciex Analyst 1.4 software.

Sample analysis of RES, ERES and BRES

Separation was performed on a ZORBAX SB-CN column (4.6 x 250 mm. 5 µm: Agilent Technologies, US) after a sample injection volume of 100 µl. The mobile phase consisted of methanol and KPO_4 buffer (pH 7.0, I=0.02) at a ratio of 2:1. Flow rate was set to 1 ml/minute and all peaks were eluted within 12 minutes. Fluorometric detection was performed using an excitation/emission setup of 530/580 nm for RES analysis and 465/540 nm for ERES and BRES analysis. The method was validated to LLOQs for RES, ERES and BRES of 0.45, 42

and 3.6 nM, respectively. BRES was used as internal standard for ERES activity analysis and vice versa.

Sample analysis of DFN and 4DFN/5DFN

Analyses of DFN and its metabolites were performed using a modified version of the method described by Kaphalia *et al* (Kaphalia *et al*., 2006). Briefly, samples were separated on a Hypersil Gold C_{18} column (4.6 x 250 mm: 5 µm particle size: Thermo Scientific, UK) after a sample injection volume of 100 µl. The mobile phase consisted of CH_3CN and 0.75 mM sodium acetate buffer, pH 5.0 at a ratio of 2:3. All peaks were isocratically eluted within 14 minutes at a mobile phase flow rate of 1 ml/minute, and detected using UV at 280 nm. A single unidentified peak eluted at 6.25 minutes was assumed to be 5DFN (Kaphalia *et al*., 2006). No authentic standard for 5DFN was commercially available but as the chromatophoric difference between 5DFN and 4DFN is presumed negligible, 4DFN was used as the reference. This practice has successfully been used in previous studies and was verified by controlling the mass balance (Cummins *et al*., 2002). The method was validated to LLOQs of 20 nM and 10 nM for DFN and 4DFN/5DFN, respectively.

Sample analysis of DXM and DXO

Analyses of DXM and DXO were performed using a modified version of the method described by Yu (Yu and Haining, 2001). Briefly, samples were isocratically separated on a ReproSil 100 Phenyl column (4.6 x 250 mm: 5µm particle size: Dr. Maisch GmbH, Germany) after a sample injection volume of 100 µl. The composition of the mobile phase was 50% 0.01 M potassium phosphate buffer, pH 5.7 (pH adjusted with 99.9% H_3PO_4) and 50 % CH_3CN and MeOH (5:4). All peaks were eluted within 14 minutes. The mobile phase flow rate was set to 1 ml/minute and fluorometric detection was performed using wavelengths of 280 nm

excitation and 310 nm emission. The method was validated to LLOQs of 5.2 nM and 5.1 nM for DXM and DXO, respectively.

Sample analysis of EMEL, NMEL and MEL

Analyses of EMEL, NMEL and MEL were performed using the method described by Andersson *et al*. (Andersson *et al*., 2005). Briefly, LC separations were performed on a revered-phase HyPURITY C_{18} analytical column (100 mm x 2.1 mm i.d ., 5 µm; ThermoQuest, Runcorn, UK) at 40ºC. The mobile phase consisted of 10% CH_3CN, 5 µM acetic acid and 10 mM ammonium acetate, resulting in a solvent with approximately pH 5. Samples were isocratically eluted at a flow rate of 0.67 ml/minute and all peaks were eluted within five minutes. Samples were detected using MS operated under the following conditions: turbo heater temperature (550°C), nebulizer gas (GS1) at 60 pounds per square inch gauge (psig), turbo gas (GS2) at 70 psig, curtain gas at 30 psig and an electrospray voltage of 4 kV in positive mode. The orifice voltage was set at 81 V, collision energy at 33 V and collision-activated dissociation gas at 10 psig. The multiple reaction monitoring transitions of the precursor ions $(M + H)^+$ to the corresponding product ions were *m/z* 458.2 to 198.2, 446.1 to 249.1 and 430.1 to 233.3 for EMEL, NMEL and MEL, respectively.

Sample analysis of FLU and 2FLU

Analyses of FLU and 2FLU were performed using a modified version of the method described by Leibinger and Kapàs (Leibinger and Kapas, 1996). Briefly, 50 µl of sample were injected and separated on a Hypersil Gold C_{18} column (4.6 x 250 mm; 5µm: Thermo Scientific, UK). The mobile phase consisted of H_2O, CH_3CN and methanol (45:35:25) at a flow rate set to 1.5 ml/minute. All peaks were eluted within 10 minutes. Eluted samples were

DMD Fast Forward. Published on September 29, 2008 as DOI: 10.1124/dmd.108.021477
This article has not been copyedited and formatted. The final version may differ from this version.

detected by UV at 300 nm and the method was validated to LLOQs of 80 nM and 60 nM for FLU and 2FLU, respectively.

Data analysis

Protein binding

The fraction unbound (f_u) at optimal protein concentration under incubation conditions was calculated by dividing the substrate concentration after filtration ([C_u]), corrected for unspecific binding to filter (f_{fb}), with unfiltered substrate concentration ([C]) (eq. 1 and eq. 2).

$$f_u = \left(\frac{[C_u]}{(1 - f_{fb}) \cdot [C]} \right) \quad \text{eq. 1}$$

$$f_{fb} = 1 - \left(\frac{[C_{ub}]}{[C_b]} \right) \quad \text{eq. 2}$$

where [C_{ub}] is the concentration after filtration and [C_b] is the concentration before filtration, measured in the absence of proteins.

Initial formation rate of metabolite method

The rates of metabolite appearance at different substrate concentrations were calculated by plotting metabolite concentration versus time. Formation rates were normalized to protein concentration and the Michaelis-Menten equation (eq. 3) was fitted by non-linear regression to formation rate vs. free substrate concentration.

$$v = \frac{V_{\max} \cdot [C_{uinc.}]}{K_m + [C_{uinc.}]} \quad \text{(eq. 3)}$$

where v is the formation rate, V_{max} is the theoretical maximum formation rate, K_m is the unbound substrate concentration at half the theoretical maximum formation rate and [$C_{uinc.}$] is the free substrate concentration ([$C_{uinc.}$] = [C] · f_u).

The unbound intrinsic clearance (CL_{int}) was calculated by dividing V_{max} by K_m (eq. 4).

DMD Fast Forward. Published on September 29, 2008 as DOI: 10.1124/dmd.108.021477
This article has not been copyedited and formatted. The final version may differ from this version.

$$CL_{\text{int}} = \frac{V_{\max}}{K_m} \qquad \text{(eq. 4)}$$

When more than one reaction was followed (DFN reaction), the sum of the individual CL_{int} values were calculated to obtain a total CL_{int}.

Multiple depletion curves method

Two models were used to describe the rate of substrate depletion. One, not correcting for EAC (MDCM), is given by eq. 5, and one, correcting for EAC described as a mono exponential decay (MDCM+*ke*), is given by eq. 6.

$$-\frac{d[C]}{dt} = v = \frac{v_{\max} \cdot [C]}{k_m + [C]} \qquad \text{(eq. 5)}$$

$$-\frac{d[C]}{dt} = v = \left(\frac{v_{\max} \cdot [C]}{k_m + [C]}\right) \cdot e^{-k_e \cdot t} \qquad \text{(eq. 6)}$$

where v_{max} is the theoretical maximum depletion rate, k_m is the substrate concentration at half the theoretical maximum depletion rate, [C] is the substrate concentration and k_e is the enzyme activity change constant.

The parameters, v_{max} and k_m, were estimated by simultaneous fitting of the equations to all concentration time profiles using non-linear regression. The regression was performed with a weighting scheme of $1/([C]^2)$.

V_{max} was obtained by dividing v_{max} with the protein concentration used in incubation (C_p) (eq. 7) and K_m was calculated by multiplying k_m with f_u (eq. 8). CL_{int} was then calculated in the same way as for the IFRMM by eq. 4.

$$V_{\max} = \frac{v_{\max}}{C_p} \qquad \text{(eq. 7)}$$

$$K_m = k_m \times f_u \qquad \text{(eq. 8)}$$

DMD Fast Forward. Published on September 29, 2008 as DOI: 10.1124/dmd.108.021477
This article has not been copyedited and formatted. The final version may differ from this version.

***"In vitro* $t_{½}$" method**

The depletion data were also used to determine CL_{int} with the $T_{½}M$ by fitting a first order of disappearance to a single selected depletion data set (eq. 9). A first order of disappearance is obtained by setting [*C*] = 0 in the denominator of eq.3, which is a fair approximation when [*C*] is negligible compared to K_m.

$$C_t = C_0 \cdot e^{-k \cdot t} \qquad \text{(eq. 9)}$$

where C_t is the concentration at time t and *k* is the disappearance rate constant.

CL_{int} was then calculated by dividing the disappearance rate constant with C_p and f_u (eq. 10).

$$CL_{\text{int}} = \frac{k}{C_p \times f_u} \qquad \text{(eq. 10)}$$

The determinations were done using the data set with the lowest available C_0 for each substrate. Further, in consideration of the risk of consistently using a fixed C_0 at 1 µM, as commonly adopted, a second determination was done for those reactions where such a data set was available.

All analyses of kinetic data were performed using WinNonlin Professional software V4.0 (Pharsight Corp.,CA). For evaluation and comparison of the goodness of fit for the different methods, Akaike information criterion, visual examination of data, residual plots and the precision of parameter estimation were used.

Monte Carlo simulations

A limited analysis of the MDCM robustness, *i.e.* accuracy and precision, was conducted to further investigate the performance of the method. The experimental variables included in the

analysis were the distribution of C_0 in relation to K_m and the relative turnover during the incubation. A similar analysis was conducted to investigate the size of the estimation error related to the $T_{½}M$ when using a suboptimal C_0. In addition, the impact of EAC was investigated.

In both the MDCM and $T_{½}M$ simulations, simulated data were generated according to eq. 6 by using the Runge-Kutta algorithm to solve values from the differential equation. In the precision study, when determining the propagation of errors (noise) from measured data into the final parameters, Monte Carlo simulations were performed with a Gaussian noise added to the generated data points. To determine a relevant noise level, a sample standard deviation study of the experimental raw data (concentrations) available was done prior to the simulations. In the experiments, the concentrations were measured in sets of five and from each set a standard deviation was calculated. Totally 120 standard deviations were determined in this way. It could be concluded from these steps that the relative standard deviation was similar over the whole concentration range with an average value of 0.073. A level of noise giving this relative standard deviation was applied in the above described Monte Carlo simulations.

Parameters were estimated from the generated data by non-linear regression carried out by an in house developed Visual Basic program using Levenberg-Marquardts curve fit algorithm linked to the Runge-Kutta algorithm for the numerical solution of the differential equation.

In the Monte Carlo simulation exercises, data points were weighted by the inverse of the standard deviation in the fittings, and the standard deviation for the individual estimates was determined. 100 simulations were made for each parameter combination. The mean and the

coefficient of variation of the 100 individual parameter estimates, respectively, were used as measures of accuracy and precision.

MDCM

The simulations were, in analogy with the experimental setup, performed using three starting concentrations (High=10, Medium=1 and Low=0.1 µM) at each parameter combination. Data at eight equidistant time points in a time interval [0, $t_{inc.}$] for a number of V_{max} and K_m combinations and with k_e = 0 were generated and the precision was determined according to the procedure described above in analogy to eq. 6. The parameter values used in combinations were 0.5, 0.05 and 0.005 µM/minute for V_{max} and 50, 5 and 0.5 µM for K_m. $t_{inc.}$ was 60 minutes in all simulations. To normalize the parameters, initial concentrations were expressed as C_0/K_m and V_{max} was divided by the high initial concentration (=10) to obtain a relative turnover expressed in percent per minute (% min^{-1}).

$T_{½}$M

The sensitivity in the parameter estimation to the inherent approximation in eq. 9 as well as the relative turnover of substrate was investigated. Data at eight equidistant time points in a time interval [0, $t_{inc.}$] for a number of C_0, V_{max}, K_m and k_e combinations were generated in analogy to eq. 6. $CL_{int,est.}$ was then estimated by fitting eq. 9 to these data and accuracy in the prediction estimate was expressed as the ratio of $CL_{int,est.}$ and $CL_{int,true}$ (*i.e.* V_{max} / K_m). The precision was then determined according to the procedure described above. Since $t_{inc.}$ has an impact on the absolute turnover, $CL_{int,true}$ was converted to *in vitro* half life ($t_{½}$) using eq. 11

$$t_{½} = \frac{\ln 2}{CL_{\text{int}}} \qquad \text{(eq. 11)}$$

and then made unit less by dividing $t_{½}$ by $t_{inc.}$, giving the relative turnover ($t_{½}/t_{inc.}$). Similarly, the initial concentrations were expressed as C_0/K_m. The parameter values used in combinations were 0.4, 0.2, 0.1, 0.05, 0.02, 0.01, 0.005 and 0.002 ml/mg/minute for $CL_{int.true}$, representing a $t_{½}$ range of 1.7-350 minutes, 1, 0.5, 0.2 and 0.1 for C_0/K_m and 0, 0.005, 0.01 and 0.02 min^{-1} for k_e. t_{inc} was fixed to 60 minutes in all simulations.

Results

Protein concentrations in incubation, the free fractions in incubation media and the loss of enzyme activities are summarized in Table 1. Unspecific binding to the filter (f_{fb}) used in the protein binding assay ranged from none detected (n.d.) to 0.68 (BRES 0.68, DFN n.d., DXM 0.19, EMEL 0.05, ERES 0.21, FLU 0.14, NMEL n.d.). No unspecific adhesion to laboratory equipment was observed. All compounds, except BRES, were chemically stable under incubation conditions. Enzyme activity (Figure 2) ranged from no observable decline (ERES) to an approximate 65% loss (BRES). An increase of the reaction velocity was observed for the two reactions conducted in porcine liver S1 fractions (EMEL and NMEL).

Enzyme kinetics

Parameters determined with the IFRMM

Primary data from the IFRMM assays are displayed in Figure 3 and the result is shown in Table 2. IFRMM data for all reactions showed monophasic, Michaelis-Menten behavior and no more complex models were necessary to describe the data. V_{max} values covered more than three orders of magnitude from 12.0 (BRES to RES) to 42800 nmol/minute/mg protein (EMEL to MEL). The K_m values covered more than four orders of magnitude from 0.0937 µM (BRES reaction) to 4710 µM (EMEL reaction). For DFN, where two metabolites were formed, the mean of 4DFN and 5DFN K_m values and the sum of the V_{max} values of the individual reactions were used in further comparisons between the IFRMM and the MDCM. The K_m values for these two reactions were very similar making this approximation reasonable. CL_{int} values, calculated from V_{max} and K_m determinations, covered approximately two orders of magnitude from 9.10 (EMEL reaction) to 836 ml/minute/g protein (DXM reaction).

DMD Fast Forward. Published on September 29, 2008 as DOI: 10.1124/dmd.108.021477
This article has not been copyedited and formatted. The final version may differ from this version.

Parameters determined with the MDCM

The data was well described by the given equations in the method sections. More complex models, e.g. two enzymes model, were also tested but did not converge. Primary data from MDCM metabolic investigations are shown in Figure 4. Results from determinations made with the MDCM (eq. 5) are shown in Table 2. V_{max} covered more than four orders of magnitude from 11.8 (dealkylation of BRES to RES) to 36100 nmol/minute/mg protein (ester hydrolysis of EMEL to MEL). The K_m values covered four orders of magnitude from 0.179 (BRES) to 2340 µM (EMEL). CL_{int} values, calculated from V_{max} and K_m determinations, covered two orders of magnitude from 1.55 (EMEL) to 311 ml/minute/g protein (ERES). The result from determinations made with the MDCM including EAC (MDCM+k_e) (eq. 6) is shown in Table 2. V_{max} covered three orders of magnitude from 26.9 (BRES to RES) to 46900 nmol/minute/mg protein (EMEL to MEL). The K_m values covered four orders of magnitude from 0.166 (BRES) to 2340 µM (EMEL). CL_{int} values, calculated from V_{max} and K_m determinations, covered two orders of magnitude from 2.01 (EMEL) to 358 ml/minute/g protein (ERES). Compensation for chemical instability was done for both methods in the case of BRES.

CL_{int} determined with the $T_{½}M$

The result from determinations made with the $T_{½}M$ (eqs. 9 and 10) is shown in Table 2. CL_{int} determinations done with the lowest available C_0 for respective substrate (BRES 0.02 µM; DFN 3 µM; DXM 5 µM; EMEL 9 µM; ERES 0.12 µM; FLU 0.5 µM and NMEL 20 µM) ranged from 8.86 (NMEL to MEL) to 71.5 ml/minute/g protein (ERES to RES). A second analysis, with a C_0 close to 1 µM, could be performed for FLU (1.4 µM, data not shown),

BRES (1 µM) and ERES (1 µM). This resulted in reductions in CL_{int} estimates of approximately 1.5-fold for the FLU reaction and 3-fold for the BRES and ERES reactions.

Monte Carlo simulations

Accuracy and precision analysis of the MDCM

The accuracy and precision of the estimates (V_{max} and K_m) were good for six of the nine tested combinations of relative initial concentration (C_0/K_m) and maximal relative turnover (% min^{-1}). Of the remaining three data sets, two suffered from poor estimates and in one, the regression did not converge (Table 3). The best accuracy in estimates (1.00 to 0.97) was obtained for the highest relative initial concentration series (20-2-0.2), even though the precision decreased at the lowest tested relative turnover (0.05 % min^{-1}). High relative turnover (5 % min^{-1}) was also related to good accuracy in the estimations (1.00 to 1.16). At the lowest relative initial concentration and relative turnover, estimations were not possible.

Accuracy and precision analysis of the $T_{½}M$

The accuracy (*estimation error (%)*) of CL_{int} estimates using the $T_{½}M$ was highly dependent both on initial concentration-relative K_m (C_0/K_m) and relative turnover, *i.e.* half life divided by time of incubation ($t_{½}/ t_{inc.}$) (Figure 7A). The accuracy decreased rapidly with increasing C_0/K_m and $t_{½}/ t_{inc.}$ ratios. The C_0/K_m ratio of 1 showed a bias greater than 40% at relatively low $t_{½}/ t_{inc.}$ ratios (>0.3). The precision was only dependent on relative turnover and decreased dramatically with increasing $t_{½}/ t_{inc.}$ ratios.

Effect of EAC on CL_{int} estimations using the $T_{½}M$

The effect of EAC on the accuracy (*estimation error (%)*) of CL_{int} estimates using the $T_{½}M$ was simulated for a reaction with C_0/K_m ratio of 0.1 (Figure 7B). The estimation error was

highly dependent on the EAC constant, k_e. A k_e value of 0.005, 0.01 and 0.02 (representing an approximate loss of activity after 60 minutes of 25, 45 and 70%, respectively) resulted in a bias of 10, 15 and 40 %, respectively. The estimation error was essentially independent of the relative turnover.

Discussion

The major objective of this study was to validate the MDCM in terms of accuracy and precision in estimating CL_{int} as well as the underlying kinetic parameters, V_{max} and K_m, using the conventional IFRMM as a reference. The validation was done both through experimental work and by means of Monte Carlo simulations. A comparison was also made with the simple $T_{½}M$. The latter method was also explored in terms of its sensitivity to the basic assumption inherent in the method, *i.e.* start concentration $C_0 << K_m$. A secondary aim was to explore the impact of a change in enzyme activity during the incubation on the parameter estimates, and the possibility to account for this in the data analysis.

Results from the MDCM were in good overall agreement with those from the traditional IFRMM in its determinations of V_{max}, K_m and CL_{int} (Figure 5). With few exceptions (K_m and CL_{int} value for DXM reaction) all the estimated parameters were within or almost within a 2-fold difference. The practice of regarding multiple kinetic pathways with equivalent K_m values as a single reaction, described by that K_m value and the sum of all individual V_{max} values, was valid in the case of DFN. The parameter values estimated by the MDCM corresponded very well with the combined values of the 4DFN and 5DFN reactions derived from the IFRMM. The inconsistency seen in the case of DXM may be explained by an influence of N-demethylation to 3-methoxymorphinan. This reaction has previously been reported to be a minor metabolic pathway in Sprague-Dawley rats but may influence the overall parameters estimated by the MDCM (Kerry *et al.*, 1993). In addition, the IFRMM results showed a general pattern of biphasic behavior (Figure 3D) indicating that a second enzymatic system may contribute to the DXO formation. If so, this could also explain the discrepancy between the two methods but no support for additional systems could been found

in the literature. The IFRMM could not be used as a reference to MDCM for FLU and NMEL since the measured metabolites surprisingly only represented 40% and 20%, respectively, of the total disappearance. A recent study identified several metabolites in rat supporting the argument that FLU are metabolized via multiple pathways (Tevell *et al*., 2006). To date, no such results have been presented for NMEL. However, this illustrates the strength with the MDCM method when the main purpose is to estimate the overall enzyme kinetic profile, *i.e*. total V_{max}, apparent K_m and total CL_{int}, especially for new chemical entities when the metabolism of the compounds is not fully characterized and the metabolic pathways are not known. When multiple kinetic pathways are present, the MDCM provides useful information of the overall kinetics without prior knowledge of metabolic pathways. These "hybrid" parameters can then be used *e.g.* to scale clearance and to predict non-linearity *in vivo*.

As expected, the Monte-Carlo simulations conducted to investigate the robustness of the MDCM showed that optimal conditions were met when the initial concentrations covered K_m and the relative turnover was high. A more interesting finding was that these two factors compensated for each other under sub-optimal conditions. Briefly, if the C_0 range was favorable it could, to some extent, compensate for a low relative turnover and vice versa (Table 3). This suggests that it is not absolutely necessary to include a concentration well above K_m for accurate estimations as long as the turnover is sufficiently high. This is highly relevant as solubility issues often prevent the use of concentrations sufficiently high to reach V_{max} when using the IFRMM. For the opposite situation, *i.e.* for compounds with a low turnover, an advantageous C_0 range could still generate accurate parameter estimations as was demonstrated for the data set with the lowest relative turnover (0.05 % min^{-1}).

CL_{int} determinations made with the $T_{½}M$ using available data sets with the lowest C_0 were essentially consistent with the results from the MDCM (Figure 6A). The issue of

DMD Fast Forward. Published on September 29, 2008 as DOI: 10.1124/dmd.108.021477
This article has not been copyedited and formatted. The final version may differ from this version.

conducting the $T_{½}M$ at a fixed C_0 was well illustrated by the decrease in CL_{int} estimates for the three compounds with low K_m (BRES, ERES and FLU) when using a C_0 close to 1.0 μM (Figure 6B). The simulation study confirmed this and also showed the significance of turnover (Figure 5A). High relative turnover reduced the effect of a suboptimal C_0. This is due to the fast decline in concentration bringing the substrate concentration quickly into the linear (*i.e.* monoexponential) concentration range. Experimentally, this was seen in the case of DXM where the C_0 value for the lowest data set were close to the apparent K_m for the reactions but the steep depletion curve still enabled an accurate determination with the $T_{½}M$. Overall, the simulation study clearly illustrated that the $T_{½}M$ is applicable and highly appropriate when C_0 is negligible in comparison to K_m ($C_0/K_m \leq 0.1$), although the accuracy of the method decreased slightly at lower turnover (>1). Systems with higher C_0/K_m ratios were associated with increased errors and were more susceptible to low turnover. It should also be highlighted that the precision was only dependent on turnover and increased dramatically with higher $t_{½}/t_{inc.}$ ratios. This is logical, as low turnover results in a low signal to noise ratio.

The secondary objective of this study was to investigate the impact of EAC on the parameter estimations. The intent of the experimental part was to estimate the degree of loss in activity to be expected when performing the depletion assays, and to identify possible differences between the enzymatic systems used. Since the potential effect of the substrates on the loss of enzyme activity was not covered by this experimental setup, the data could not be directly used as k_e in the MDCM regression analysis. Large differences in instability were seen and the level of enzyme activity loss after 60 minutes of incubation stress ranged from zero to over 60%, reflecting the different enzyme systems and isoforms involved in the metabolism of the substrates in the study. This variability also indicates that individual investigations must be conducted, as there is no generally applicable compensation for EAC. For the reactions

using liver S1 fractions, the activity increased after the first measurement, possibly because the enzymes in the incubation matrix were not fully recovered from the cooling process before the first reaction was started. The correction of EAC in the MDCM had an inconsistent effect on the primary variables (V_{max} and K_m) but improved the overall accuracy of CL_{int} (Figure 5) compared to the IFRMM. The precision, however, decreased for CL_{int} while it increased for K_m. No clear trend for V_{max} was seen. Overall, the correction of EAC improved the agreement of the data with the IFRMM. Further support of our findings regarding the effect of EAC was provided by the simulations with the $T_{½}M$ (Figure 7B). The impact of EAC could, to a major extent, explain the remaining differences between the $T_{½}M$ and the MDCM+k_e. The observed estimation error appears to be the sum of the effects of relative turnover and EAC. This may be explained by the fact that the EAC systematically decreases all systems proportionally over time. As the CL_{int} estimations using the MDCM-k_e were in better overall agreement with the IFRMM than the MDCM (as seen in Figure 5: panel E and F), we consider that the $T_{½}M$ determinations also would benefit from an EAC correction. The reasons for EAC can be numerous, such as enzyme degradation, damage from NADPH generated radicals, co-factor depletion and substrate and/or metabolite inhibition. In simpler enzyme systems such as cell fractions and purified enzymes, the risk of inhibition is greater than in the *in vivo* situation, as phase II metabolism is inactive or missing (Masimirembwa *et al*., 2003; Jones *et al*., 2005). It has also been reported that enzyme degradation positively correlates with increased enzyme concentration (Jones and Houston, 2004). The latter is important to keep in mind as increasing the protein concentration in order to boost substrate turnover is appealing when using substrate depletion approaches.

Results from the MDCM are specific for the enzymatic system under study and the method can therefore be adapted to the purpose. When applied to mixed enzyme systems, the

method will provide information on the overall kinetics, where the parameters obtained represent a conglomerate of all reactions present. Like all depletion based methods the MDCM has difficulties to distinguish individual enzymatic routes. If this is the purpose, the method could very well be applied for single enzyme systems (*e.g.* recombinant CYPs), although not studied here. When the objective of a study is to estimate overall enzyme kinetics, the MDCM is superior to the IFRMM. In early Drug discovery, the metabolic fate of compounds is not known which automatically disqualifies the use of the IFRMM. Still, for compounds with known metabolic pathways (*e.g.* drug candidates), the IFRMM requires chemical synthesis and the development of quantitative bioanalytical methods for all of the metabolites. Even so, the IFRMM suffers from potential drawbacks such as sequential metabolism of the primary metabolites, which needs to be compensated for. In contrast to the $T_{½}M$, the MDCM can be used to calculate V_{max} and K_m and is not restricted by potential errors related to assumptions that may affect the validity of the method. As with depletion methods in general, however, the MDCM is dependent on a certain degree of turnover relative the experimental noise.

The overall conclusion from this study is that the MDCM can be used to precisely and accurately estimate enzymatic variables governing overall metabolism. We also expect the method to be widely applicable, as the numerical range for the variables studied (V_{max}, K_m and CL_{int}) were large and the Monte Carlo simulation study demonstrated that factors like C_0 range and metabolic turnover compensate for each other under sub-optimal conditions. Correction for EAC was possible and improved the accuracy in the estimations. Although the experimental setup used in this study was fairly sample rich and hence not optimal for screening purposes, it is still expected that the method will perform well with a reduced

number of samples. An extended study, however, is needed to find the optimal experimental setup for such an application.

Finally, the MDCM may potentially be used in a wide range of applications, from pure enzyme kinetics to *in vitro*-based predictions of the pharmacokinetics of compounds with multiple and/or unknown metabolic pathways.

References

Andersson S, Hofmann Y, Nordling A, Li XQ, Nivelius S, Andersson TB, Ingelman-Sundberg M and Johansson I (2005) Characterization and partial purification of the rat and human enzyme systems active in the reduction of N-hydroxymelagatran and benzamidoxime. *Drug Metab Dispos* **33:**570-578.

Berson A, Wolf C, Chachaty C, Fisch C, Fau D, Eugene D, Loeper J, Gauthier JC, Beaune P, Pompon D and et al. (1993) Metabolic activation of the nitroaromatic antiandrogen flutamide by rat and human cytochromes P-450, including forms belonging to the 3A and 1A subfamilies. *J Pharmacol Exp Ther* **265:**366-372.

Bousquet-Melou A, Laffont CM, Laroute V and Toutain PL (2002) Modelling the loss of metabolic capacities of cultured hepatocytes: application to measurement of Michaelis-Menten kinetic parameters in in vitro systems. *Xenobiotica* **32:**895-906.

Carlile DJ, Hakooz N, Bayliss MK and Houston JB (1999) Microsomal prediction of in vivo clearance of CYP2C9 substrates in humans. *Br J Clin Pharmacol* **47:**625-635.

Clement B and Lopian K (2003) Characterization of in vitro biotransformation of new, orally active, direct thrombin inhibitor ximelagatran, an amidoxime and ester prodrug. *Drug Metab Dispos* **31:**645-651.

Cummins CL, Jacobsen W and Benet LZ (2002) Unmasking the dynamic interplay between intestinal P-glycoprotein and CYP3A4. *J Pharmacol Exp Ther* **300:**1036-1045.

Eriksson UG, Bredberg U, Hoffmann KJ, Thuresson A, Gabrielsson M, Ericsson H, Ahnoff M, Gislen K, Fager G and Gustafsson D (2003) Absorption, distribution, metabolism, and excretion of ximelagatran, an oral direct thrombin inhibitor, in rats, dogs, and humans. *Drug Metab Dispos* **31:**294-305.

Fau D, Eugene D, Berson A, Letteron P, Fromenty B, Fisch C and Pessayre D (1994) Toxicity of the antiandrogen flutamide in isolated rat hepatocytes. *J Pharmacol Exp Ther* **269:**954-962.

Houston JB and Carlile DJ (1997) Prediction of hepatic clearance from microsomes, hepatocytes, and liver slices. *Drug Metab Rev* **29:**891-922.

Ito K and Houston JB (2005) Prediction of human drug clearance from in vitro and preclinical data using physiologically based and empirical approaches. *Pharm Res* **22:**103-112.

Iwatsubo T, Hirota N, Ooie T, Suzuki H, Shimada N, Chiba K, Ishizaki T, Green CE, Tyson CA and Sugiyama Y (1997) Prediction of in vivo drug metabolism in the human liver from in vitro metabolism data. *Pharmacol Ther* **73:**147-171.

Jones HM and Houston JB (2004) Substrate depletion approach for determining in vitro metabolic clearance: time dependencies in hepatocyte and microsomal incubations. *Drug Metab Dispos* **32:**973-982.

Jones HM, Nicholls G and Houston JB (2005) Impact of end-product inhibition on the determination of in vitro metabolic clearance. *Xenobiotica* **35:**439-454.

Kaphalia L, Kaphalia BS, Kumar S, Kanz MF and Treinen-Moslen M (2006) Efficient high performance liquid chromatograph/ultraviolet method for determination of diclofenac and 4'-hydroxydiclofenac in rat serum. *J Chromatogr B Analyt Technol Biomed Life Sci* **830:**231-237.

Kerry NL, Somogyi AA, Mikus G and Bochner F (1993) Primary and secondary oxidative metabolism of dextromethorphan. In vitro studies with female Sprague-Dawley and Dark Agouti rat liver microsomes. *Biochem Pharmacol* **45:**833-839.

Kobayashi K, Urashima K, Shimada N and Chiba K (2002) Substrate specificity for rat cytochrome P450 (CYP) isoforms: screening with cDNA-expressed systems of the rat. *Biochem Pharmacol* **63:**889-896.

Leibinger J and Kapas M (1996) New and validated high-performance liquid chromatographic method for determination of hydroxyflutamide in human plasma. *J Pharm Biomed Anal* **14:**1377-1381.

Ludden TM (1991) Nonlinear pharmacokinetics: clinical Implications. *Clin Pharmacokinet* **20:**429-446.

Masimirembwa CM, Bredberg U and Andersson TB (2003) Metabolic stability for drug discovery and development: pharmacokinetic and biochemical challenges. *Clin Pharmacokinet* **42:**515-528.

Obach RS (1999) Prediction of human clearance of twenty-nine drugs from hepatic microsomal intrinsic clearance data: An examination of in vitro half-life approach and nonspecific binding to microsomes. *Drug Metab Dispos* **27:**1350-1359.

Obach RS, Baxter JG, Liston TE, Silber BM, Jones BC, MacIntyre F, Rance DJ and Wastall P (1997) The prediction of human pharmacokinetic parameters from preclinical and in vitro metabolism data. *J Pharmacol Exp Ther* **283:**46-58.

Obach RS and Reed-Hagen AE (2002) Measurement of Michaelis constants for cytochrome P450-mediated biotransformation reactions using a substrate depletion approach. *Drug Metab Dispos* **30:**831-837.

Rane A, Wilkinson GR and Shand DG (1977) Prediction of hepatic extraction ratio from in vitro measurement of intrinsic clearance. *J Pharmacol Exp Ther* **200:**420-424.

Rodrigues AD (1997) Preclinical drug metabolism in the age of high-throughput screening: an industrial perspective. *Pharm Res* **14:**1504-1510.

Rostami-Hodjegan A and Tucker GT (2007) Simulation and prediction of in vivo drug metabolism in human populations from in vitro data. *Nat Rev Drug Discov* **6:**140-148.

Tang W, Stearns RA, Bandiera SM, Zhang Y, Raab C, Braun MP, Dean DC, Pang J, Leung KH, Doss GA, Strauss JR, Kwei GY, Rushmore TH, Chiu SH and Baillie TA (1999)

Studies on cytochrome P-450-mediated bioactivation of diclofenac in rats and in human hepatocytes: identification of glutathione conjugated metabolites. *Drug Metab Dispos* **27:**365-372.

Tevell A, Lennernas H, Jonsson M, Norlin M, Lennernas B, Bondesson U and Hedeland M (2006) Flutamide metabolism in four different species in vitro and identification of flutamide metabolites in human patient urine by high performance liquid chromatography/tandem mass spectrometry. *Drug Metab Dispos* **34:**984-992.

Yu A and Haining RL (2001) Comparative contribution to dextromethorphan metabolism by cytochrome P450 isoforms in vitro: can dextromethorphan be used as a dual probe for both CTP2D6 and CYP3A activities? *Drug Metab Dispos* **29:**1514-1520.

Footnotes

This work was supported by AstraZeneca R&D Mölndal, Mölndal, Sweden.

Requests to receive reprints should be sent to

Hans Lennernäs, PhD, Professor in Biopharmaceutics

Department of Pharmacy

Uppsala University

Box 580

SE-751 23 Uppsala

Sweden

e-mail: hans.lennernas@farmaci.uu.se

Legends for figures

Figure 1. Chemical structures and metabolic reactions investigated in this study.

* Specific reaction pathway unidentified.

Figure 2. Enzyme activity, displayed as percent change of initial reaction rate, versus time of incubation stress. Enzyme activity shown as mean values of triplicates with SD. **A):** Reactions catalyzed by unstable enzyme systems; benzyloxyresorufin (●), flutamide (■), diclofenac (◆), dextromethorphan (▲). **B):** Reactions catalyzed by stable enzyme systems; ethoxyresorufin (○), ethylmelagatran (□), N-hydroxymelagatran (◊).

Figure 3. Substrate saturation plots, from initial formation rate data. Actual data points and Michaelis-Menten model fitted curves are displayed. **A)** resorufin formation from benzyloxyresorufin. **B)** 4'-OH-diclofenac formation from diclofenac. **C)** 5-OH-diclofenac formation from diclofenac. **D)** dextrorphan formation from dextromethorphan. **E)** melagatran formation from ethylmelagatran. **F)** resorufin formation from ethoxyresorufin. **G)** 2-OH-flutamide formation from flutamide. **H)** melagatran formation from N-hydroxymelagatran.

Figure 4. Substrate depletion plots. Points correspond to observed concentrations. The solid lines represent model fitted data from the regression analyses using the multiple depletion curves method including correction for loss in enzyme activity (MDCM+ *ke*). **A)** benzyloxyresorufin. **B)** diclofenac. **C)** dextromethorphan. **D)** ethylmelagatran. **E)** ethoxyresorufin. **F)** flutamide. **G)** N-hydroxymelagatran.

Figure 5. Plots of kinetic parameters estimated from depletion data using the multiple depletion curves method without (MDCM) or with enzyme activity change variable

(MDCM+ k_e) versus estimations from initial formation rate data (IFRMM). The solid and the dashed lines represent the line of unity and a 2-fold range, respectively. Error bars display respective SE values. **A)** V_{max} determinations using MDCM **B)** V_{max} determinations using MDCM+k_e. **C)** K_m determinations using MDCM **D)** K_m determinations using MDCM+ k_e. **E)** CL_{int} determinations using MDCM. **F)** CL_{int} determinations using MDCM+ k_e.

Figure 6. Comparison of CL_{int} estimations determined with the multiple depletion curves method without (MDCM) (●) or with enzyme activity change variable (MDCM+ k_e) (■) versus CL_{int} values determined using the "*in vitro* $t_{½}$" method ($T_{½}M$). CL_{int} estimations are shown as mean values with SE. **A)** CL_{int} values are determined with $T_{½}M$ using the data set with the lowest initial substrate concentration available. **B)** Visualization of the effect on accuracy when using a data set close to 1 µM for the studied reactions with low K_m values.

Figure 7. Estimation error (%) in recovered CL_{int} values using the "*in vitro* $t_{½}$" method ($T_{½}M$) versus relative turnover, *i.e.* half life related to time of incubation ($t_{½}/t_{inc.}$). Error bars display SE values. **A)** Estimation error (%) dependency of relative initial concentration (C_0/K_m). C_0/K_m=0.1 (▲), C_0/K_m=0.2 (◆), C_0/K_m=0.5 (■), C_0/K_m=1 (●) **B)** Estimation error (%) dependency of enzyme activity change at C_0/K_m=0.1, described by a first order elimination constant (k_e). k_e=0.02 (Δ),k_e=0.01 (◊), k_e=0.005 (□), k_e=0 (○).

DMD Fast Forward. Published on September 29, 2008 as DOI: 10.1124/dmd.108.021477
This article has not been copyedited and formatted. The final version may differ from this version.

Table 1: Incubation validation summary showing optimal protein concentration, unbound fraction (f_u) and percent enzyme activity after 60 minutes incubation stress as change of initial reaction rate. Values shown as mean with SD (n=3).

Substrate	Optimal protein concentration (mg ml^{-1})	f_u	Enzyme activity at 60 minutes (%)
Benzyloxyresorufin	0.50	0.21 ± 0.02	34.3 ± 2.9
Diclofenac	0.50	0.85 ± 0.05	79.7 ± 2.1
Dextromethorphan	0.50	0.71 ± 0.08	75.5 ± 9.6
Ethylmelagatran	0.30	1.0 ± 0.11	129 ± 12
Ethoxyresorufin	0.125	0.61 ± 0.04	101 ± 7.8
Flutamide	0.50	0.68 ± 0.02	85.1 ± 3.8
N-hydroxymelagatran	0.30	0.90 ± 0.17	126 ± 16

Table 2: Summary for enzyme kinetic variables obtained in this study with the initial formation rate of metabolite method (IFRMM), the multiple depletion curves method without (MDCM) or with (MDCM+k_e) enzymatic activity variable (k_e) and the "*in vitro* $t_{½}$" method ($T_{½}M$). Values are shown as means with SE.

Variable	Method	Benzyloxyresorufin	Diclofenac	Dextromethorphan	Ethylmelagatran	Ethoxyresorufin	Flutamide*	N-hydroxymelagatran*
K_m (µM)	IFRMM	0.0937 ± 0.012	19.8 ± 2.1[a] 19.6 ± 2.4[b]	0.795 ± 0.13	4710 ± 2400	0.152 ± 0.016	2.48 ± 0.40	50.3 ± 5.4
	MDCM	0.179 ± 0.099	17.8 ± 2.2	5.15 ± 0.95	2340 ± 800	0.174 ± 0.038	4.03 ± 0.54	428 ± 280
	MDCM+k_e	0.166 ± 0.082	16.4 ± 1.9	3.18 ± 0.50	2340 ± 790	0.157 ± 0.038	3.76 ± 0.40	294 ± 160
V_{max} (pmol min^{-1} mg^{-1})	IFRMM	12.0 ± 0.48	668 ± 20[a] 473 ± 16[b]	665 ± 17	42800 ± 17000	71.3 ± 2.0	200 ± 7.5	318 ± 9.1
	MDCM	11.8 ± 6.8	784 ± 85	875 ± 140	36100 ± 12000	54.2 ± 7.5	282 ± 33	4090 ± 2300
	MDCM+ k_e	26.9 ± 13	1060 ± 120	1210 ± 120	46900 ± 16000	56.1 ± 10	472 ± 48	8540 ± 400
CL_{int} (ml min^{-1} g^{-1})	IFRMM	128 ± 17	33.7 ± 3.8[a] 24.2 ± 3.0[b]	836 ± 130	9.10 ± 5.9	470 ± 51	82.2 ± 14	6.32 ± 1.7
	MDCM	66.1 ± 7.5	44.0 ± 1.2	170 ± 5.9	15.5 ± 0.77	311 ± 28	70.1 ± 2.0	9.57 ± 1.4
	MDCM+ k_e	162 ± 28	64.7 ± 4.4	380 ± 31	20.1 ± 3.0	358 ± 67	125 ± 7.1	29.1 ± 8.9
	$T_{½}M^{+}$	67.6 ± 11	40.1 ± 1.2	-	16.3 ± 3.2	-	84.1 ± 4.3	8.86 ± 1.6
	$T_{½}M^{++}$	10.9 ± 5.9	-	-	-	222 ± 18	55.9 ± 1.5	-
	$T_{½}M^{+++}$	-	-	154 ± 3.2	-	71.5 ± 4.0	-	-
k_e (min^{-1})	MDCM+ k_e	0.034 ± 0.008	0.013 ± 0.002	0.025 ± 0.002	0.0094 ± 0.005	0.0061 ± 0.005	0.020 ± 0.002	0.040 ± 0.01

-, estimation not performed
[+,] estimation done at an initial concentration well below the K_m value estimated by MDCM
[++], estimation done at an initial concentration close to the K_m value estimated by MDCM
[+++], estimation done at an initial concentration greater than the K_m value estimated by MDCM
[a], diclofenac 4'-hydroxylation reaction
[b], diclofenac 5-hydroxylation reaction
*, variables obtained from IFRMM not included in method comparisons due to incomplete mass balance.

DMD Fast Forward. Published on September 29, 2008 as DOI: 10.1124/dmd.108.021477
This article has not been copyedited and formatted. The final version may differ from this version.

Table 3: Summary of the Monte Carlo simulation study investigating the robustness of the multiple depletion curves method. Accuracy and precision (estimated value/true value ± coefficient of variation) of the estimated kinetic variables, V_{max} and K_m, at different relative initial concentration levels, C_0/K_m (High-Medium-Low) and relative turnover (% min^{-1}).

	Relative turnover (% min^{-1})					
	5		0.5		0.05	
C_0/K_m (H-M-L)	K_m	V_{max}	K_m	V_{max}	K_m	V_{max}
20-2-0.2	1.0 ± 0.088	1.0 ± 0.077	1.0 ± 1.3	1.0 ± 1.1	0.99 ± 16	0.97 ± 13
2-0.2-0.02	1.0 ± 1.2	1.0 ± 1.0	0.98 ± 17	0.97 ± 15	14 ± 670	9.5 ± 680
0.2-0.02-0.002	1.2 ± 43	1.1± 41	6.9 ± 770	5.4 ± 730	*	*

* indicates that estimation was not possible

FIGURE 1

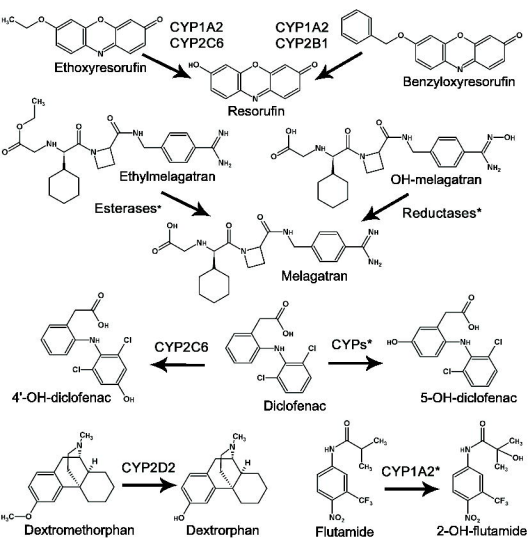
CYP1A2
CYP2C6
CYP1A2
CYP2B1
Ethoxyresorufin
Benzyloxyresorufin
Resorufin
Ethylmelagatran
OH-melagatran
Esterases*
Reductases*
Melagatran
CYP2C6
CYPs*
4'-OH-diclofenac
Diclofenac
5-OH-diclofenac
CYP2D2
CYP1A2*
Dextromethorphan
Dextrorphan
Flutamide
2-OH-flutamide

FIGURE 2

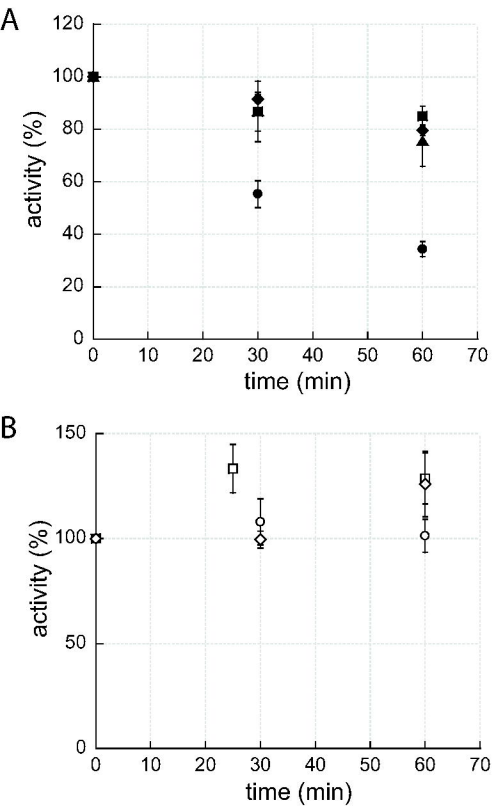

FIGURE 3

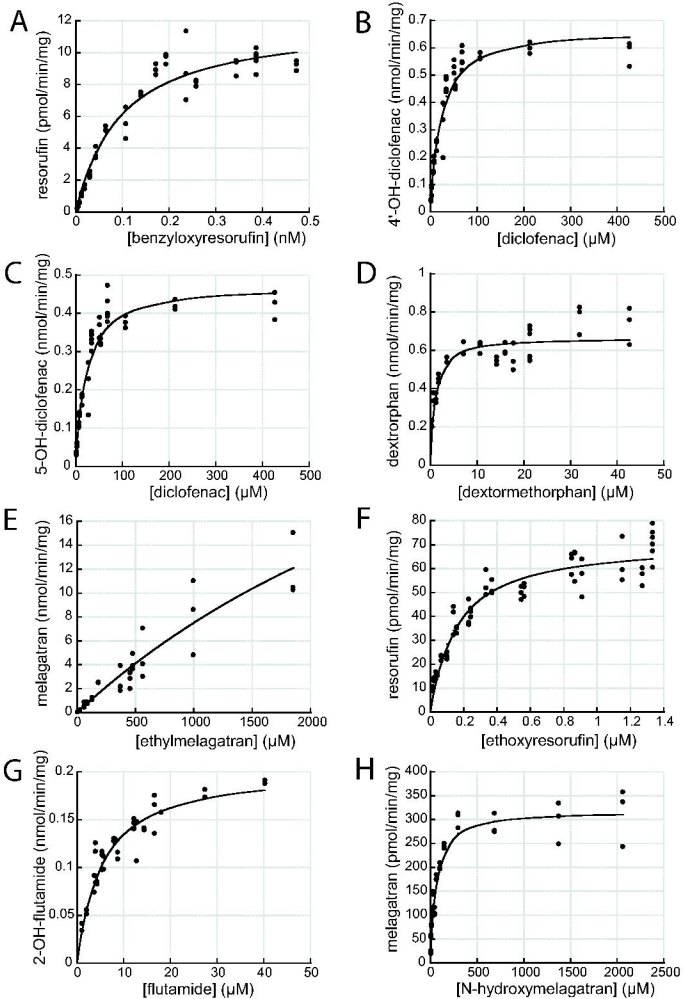
A
resorufin (pmol/min/mg)
[benzyloxyresorufin] (nM)
B
4'-OH-diclofenac (nmol/min/mg)
[diclofenac] (μM)
C
5-OH-diclofenac (nmol/min/mg)
[diclofenac] (μM)
D
dextrorphan (nmol/min/mg)
[dextormethorphan] (μM)
E
melagatran (nmol/min/mg)
[ethylmelagatran] (μM)
F
resorufin (pmol/min/mg)
[ethoxyresorufin] (μM)
G
2-OH-flutamide (nmol/min/mg)
[flutamide] (μM)
H
melagatran (pmol/min/mg)
[N-hydroxymelagatran] (μM)

FIGURE 4

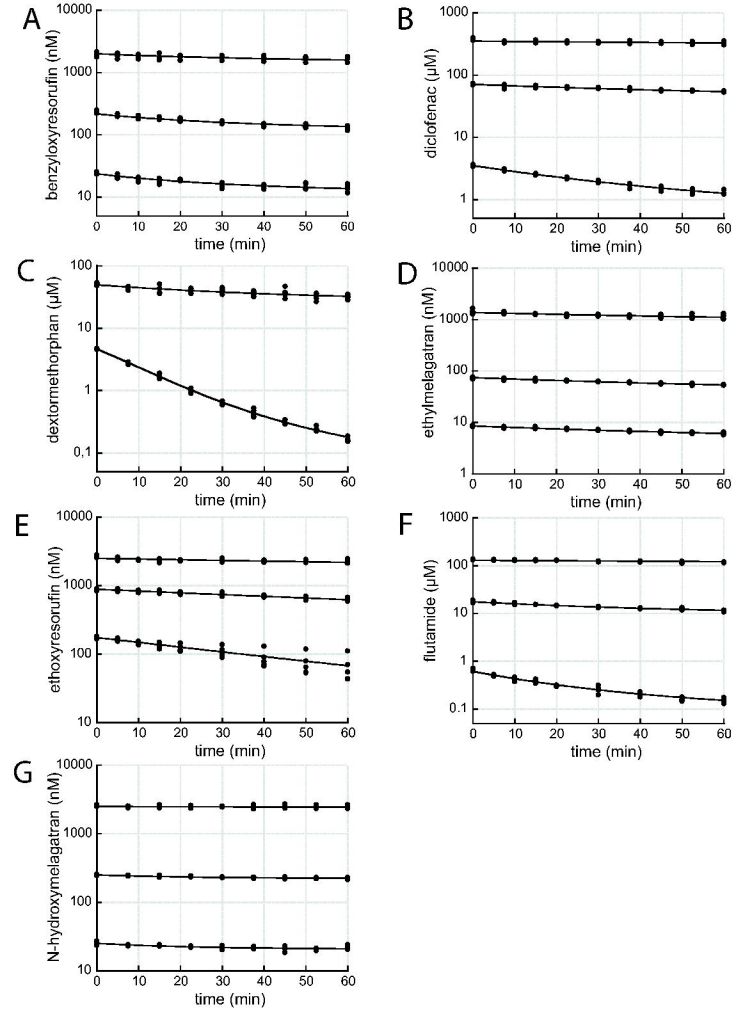
A
benzyloxyresorufin (nM)
10000
1000
100
10
0 10 20 30 40 50 60
time (min)
B
diclofenac (µM)
1000
100
10
1
0 10 20 30 40 50 60
time (min)
C
dextormethorphan (µM)
100
10
1
0,1
0 10 20 30 40 50 60
time (min)
D
ethylmelagatran (nM)
10000
1000
100
10
1
0 10 20 30 40 50 60
time (min)
E
ethoxyresorufin (nM)
10000
1000
100
10
0 10 20 30 40 50 60
time (min)
F
flutamide (µM)
1000
100
10
1
0.1
0 10 20 30 40 50 60
time (min)
G
N-hydroxymelagatran (nM)
10000
1000
100
10
0 10 20 30 40 50 60
time (min)

FIGURE 5

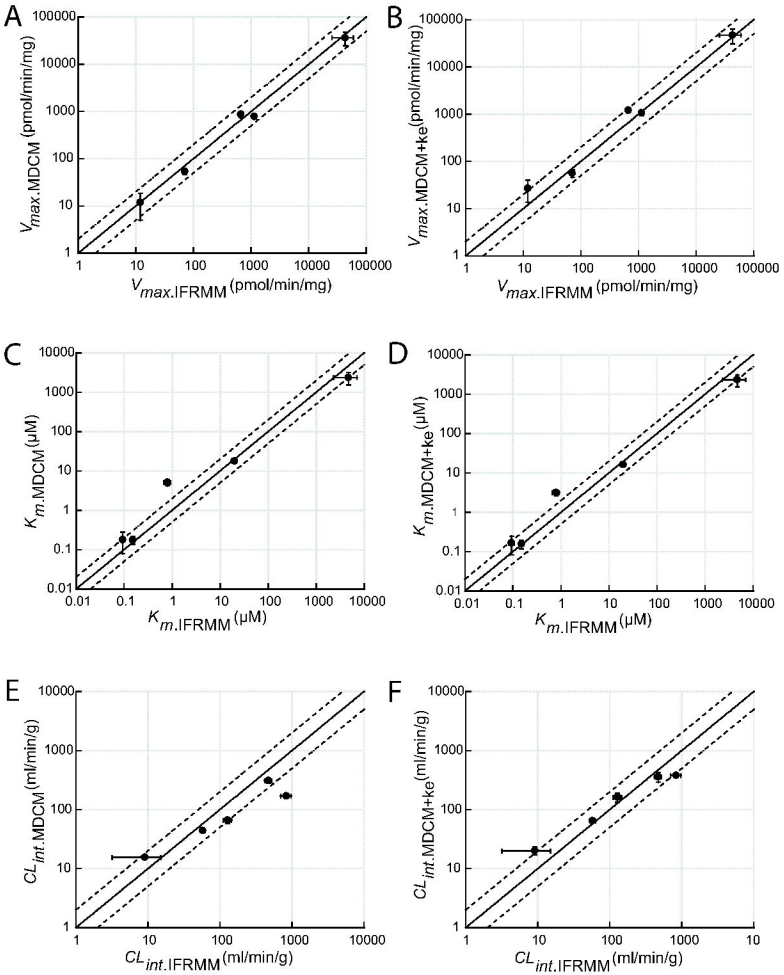
A
B
C
D
E
F
V_{max}.MDCM (pmol/min/mg)
V_{max}.MDCM+ke (pmol/min/mg)
V_{max}.IFRMM (pmol/min/mg)
K_m.MDCM (μM)
K_m.MDCM+ke (μM)
K_m.IFRMM (μM)
CL_{int}.MDCM (ml/min/g)
CL_{int}.MDCM+ke (ml/min/g)
CL_{int}.IFRMM (ml/min/g)

FIGURE 6

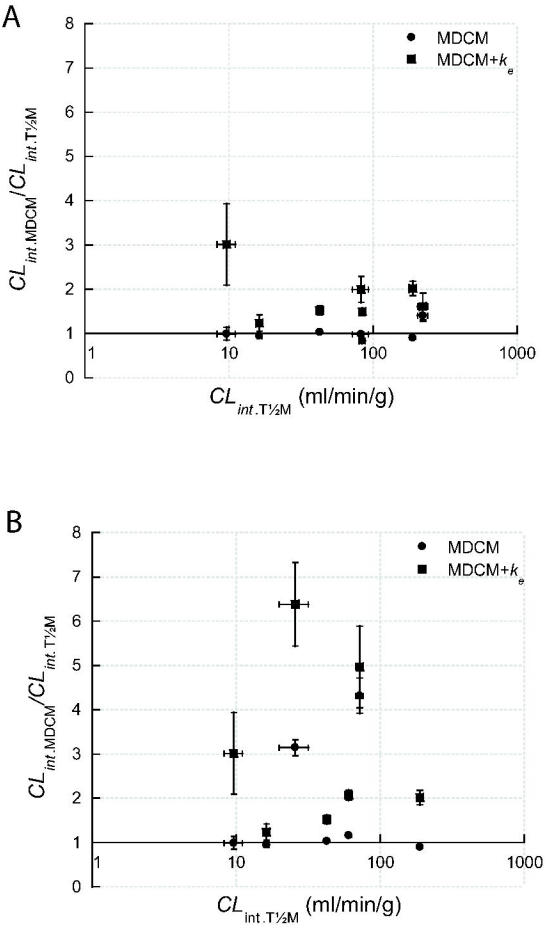
A
MDCM
MDCM+k_e
$CL_{int.MDCM}/CL_{int.T½M}$
$CL_{int.T½M}$ (ml/min/g)
0
1
2
3
4
5
6
7
8
1
10
100
1000
B
MDCM
MDCM+k_e
$CL_{int.MDCM}/CL_{int.T½M}$
$CL_{int.T½M}$ (ml/min/g)
0
1
2
3
4
5
6
7
8
1
10
100
1000

FIGURE 7

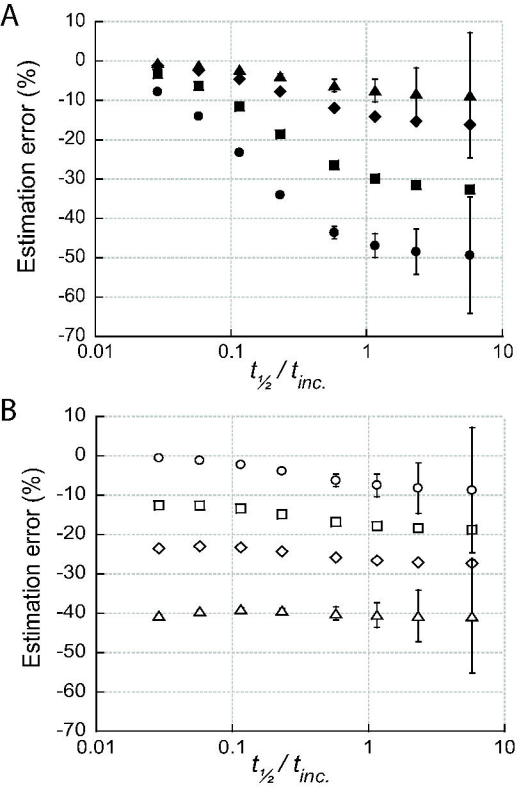
A
Estimation error (%)
10
0
-10
-20
-30
-40
-50
-60
-70
0.01
0.1
1
10
$t_{½} / t_{inc.}$
B
Estimation error (%)
10
0
-10
-20
-30
-40
-50
-60
-70
0.01
0.1
1
10
$t_{½} / t_{inc.}$